# Ultra Compact Inline E-Plane Waveguide Bandpass Filters Using Cross Coupling

**Mohottige, N., Glubokov, O., Jankovic, U. and Budimir, D.**

This is a copy of the author's accepted version of a paper subsequently published in *IEEE Transactions on Microwave Theory and Techniques*, online first 23 June 2016, DOI: 10.1109/TMTT.2016.2578329

It will be available online at:

http://dx.doi.org/10.1109/TMTT.2016.2578329

# Ultra Compact Inline E-plane Waveguide Bandpass Filters Using Cross-Coupling

Nandun Mohottige, *Member, IEEE*, Oleksandr Glubokov, *Member, IEEE*, Uros Jankovic and Djuradj Budimir, *Senior Member, IEEE*

***Abstract*—This paper presents novel ultra-compact waveguide bandpass filters that exhibit pseudo-elliptic responses with ability to place transmission zeros on both sides of the passband to form sharp roll-offs. The filters contain E-plane extracted pole sections cascaded with cross-coupled filtering blocks. Compactness is achieved by the use of evanescent mode sections and closer arranged resonators modified to shrink in size. The filters containing non-resonating nodes are designed by means of the generalized coupling coefficients (GCC) extraction procedure for the cross-coupled filtering blocks and extracted pole sections. We illustrate the performance of the proposed structures through the design examples of a third and a fourth order filters with center frequencies of 9.2 GHz and 10 GHz respectively. The sizes of the proposed structures suitable for fabricating using the low-cost E-plane waveguide technology are 38% smaller than ones of the E-plane extracted pole filter of the same order.**

***Index Terms*—Inline filters, E-plane filters, extracted pole filters, waveguide filters, generalized coupling coefficients.**

## I. Introduction

As the electromagnetic spectrum is continually populated, it is becoming increasingly important that microwave filters provide efficient frequency selectivity. Waveguide filters are widely used in fixed wireless communication, as well as for radar and satellite applications, due to their low loss and high power handling capabilities. Furthermore, the developments in such communication systems have placed stringent requirements in terms of the compactness of filtering structures. An efficient approach to achieve size reduction of waveguide filters came with successful implementations of dual-mode filters [1], which reduce the number of required resonators by half. Recent examples of these filters include [2] - [3] exploiting the use of TM modes instead of TE modes to reduce cavity lengths, and [4] introducing steps to suppress spurious modes in wider frequency ranges. Nevertheless, currently available dual mode filters have disadvantages in terms of high design complexity, as well as having time consuming and costly production.

Inserting high permittivity dielectric resonators (pucks manufactured out of currently available high performance dielectric materials) into waveguide cavities is another actively used approach to achieve size reduction; the most notable advantage of this method is the realization of extremely high quality factors. Examples of new developments in advanced filtering structures using this approach can be found in [5] - [6]. The drawbacks of using such filters include the increased design complexity, the availability of pucks with required dimensions and, furthermore, they are limited to narrow band applications. It should also be noted that the attempts to reduce losses by increasing dielectric permittivity, and by reducing resonator volume where the losses are concentrated, are limited by the increase of dielectric's tanδ.

Konishi and Uenakada first introduced the planar circuit mounted E-plane strip in [7] in order to address the high costs and design complexities that pertain to waveguide filters, in turn boosting the mass producible characteristics of the filters. However, conventional filters formed out of the planar mounted half-wavelength resonators again pose a disadvantage in terms of size, mainly lengthwise due to the cascading of the resonators. Therefore, one of the approaches that could lead to size reduction is the miniaturization of the resonators. Several such attempts at achieving compactness for this type of structures, at the same time enhancing the filter performance in terms of selectivity and attenuation at stopbands, include the use of the cross-coupled E-plane resonators [8], embedded S-shape resonators [9], and E-plane extracted pole sections (EPS) [10]. However, the septa widths required for realizing low coupling coefficients between adjacent resonators is another factor that leads to the increase in size. This paper therefore addresses this issue by expanding on the work we briefly demonstrated in [11], in return proposing a class of ultra-compact pseudo-elliptic E-plane waveguide filters for applications where space is at a premium.

## II. Ultra Compact E-plane Filtering Modules

In this section, we present two basic low-order E-plane waveguide filter structures which will be further used as building blocks for more advanced higher-order filters (see section IV).

### *A. E-plane Waveguide Singlets*

Configuration of a novel compact E-plane waveguide singlet is shown in Fig. 1. The structure is composed of two metallic inserts inside a waveguide section centred longitudinally and positioned parallel with the central E-plane, also with equal offsets from it. One of the inserts (see Fig. 1b)

Nandun Mohottige, Uros Jankovic and Djuradj Budimir are with the Wireless Communications Research Group, University of Westminster, London, W1W 6UW, United Kingdom. (e-mail: d.budimir@wmin.ac.uk).

Oleksandr Glubokov is with the Micro and Nanosystems, School of Electrical Engineering, KTH Royal Institute of Technology, Stockholm SE-100 44, Sweden. (e-mail: glubokov@kth.se).

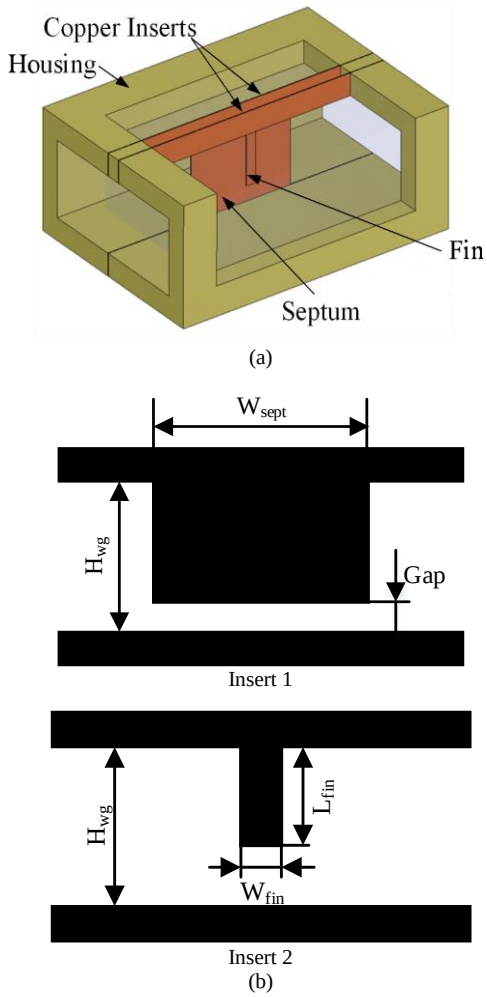


Fig. 1. Arrangement of E-plane inserts within a waveguide housing for the proposed E-plane singlet: (a) configuration of the assembled module; (b) configurations of the inserts.

consists of a single wide septum, whereas the other consists of a single fin short-circuited onto either top or bottom broad wall of the waveguide.

Essentially, the structure shown in Fig. 1, is an evanescent-mode filter configuration, since the filter operates below the cut-off frequency of the middle section as it has been narrowed by the wide septum. Moreover, though it has not been implemented here for the sake of ease of fabrication, the path behind the wide septum can be entirely eliminated, leading to characteristic evanescent mode filter cross-sectional size reduction. On the front side of the wide septum, there exist two signal paths. The main one passes through the resonators formed between the fin and the wide septum, and is active at the filter's operating frequencies. It also has fundamentally strong coupling with input and output waveguide sections due to it being centrally positioned. The other one is mainly between the fins and the adjacent sidewall, which creates spurious resonance at significantly higher frequencies.

The behaviour of the proposed structure, in its current configuration, can be represented through a schematic circuit model with three nodes, introduced by Amari and Bornemann in [12]. It consists of a positive source-load coupling due to the wide inductive septum and also has an inductive coupling for both source-resonator and resonator-load couplings due to

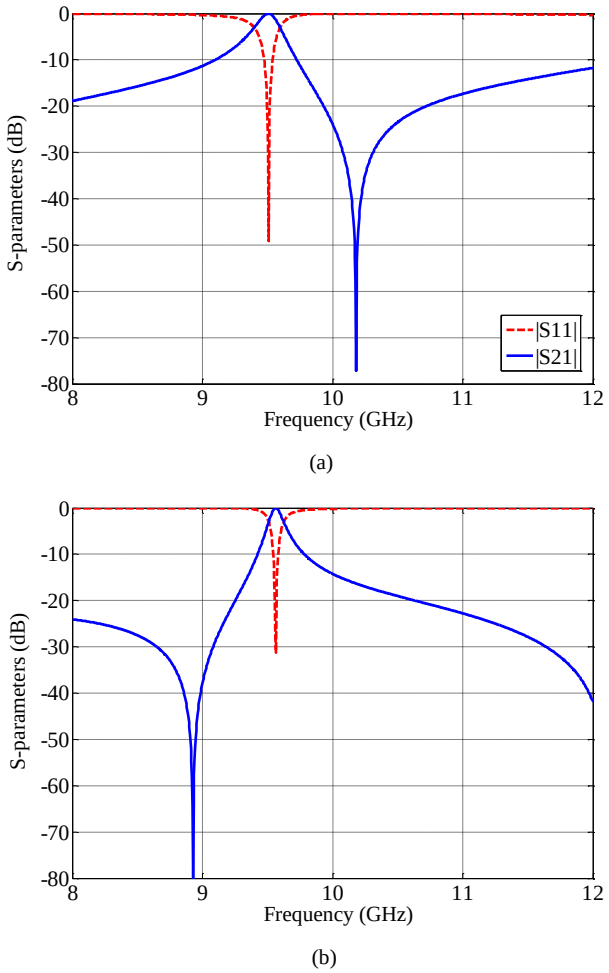


Fig. 2. S-parameters of the proposed singlet modules: (a) w/o a gap in wide septum (*Gap* = 0); (b) with a gap in wide septum (*Gap* ≠ 0).

the H-plane step discontinuity that connects the input/output terminating waveguide sections into the central evanescent mode waveguide section. Thus, the destructive interference leading towards the formation of the transmission zero occurs above the passband, as shown in Fig. 2a. In order to locate the transmission zero below the passband, it is convenient to change the bypass coupling to capacitive. This can be achieved by changing the wide septum to a wide fin by introducing a gap. As an example, the effect of this simple geometric change in the structure, without altering any other dimensions, is demonstrated by the S-parameter response in Fig. 2b.

### *B. E-plane Waveguide Doublet*

In filter applications it is also required to develop filtering modules with improved selectivity and stopband attenuation on the both sides of the passband. The singlet presented in the previous subsection can be easily modified into a 2nd-order block satisfying the requirement. A configuration of the E-plane doublet structure is shown Fig. 3a. Here, one of the inserts shown in Fig. 3b consists of two fins separated by a narrow septum, whereas the other consists of a wide fin to form a capacitive bypass coupling between the source and the load. The effect this creates can be modelled by a doublet – a

filtering module capable of generating two poles and two transmission zeros in both upper and lower stopbands [13]. However, unlike the coupling schematic of the classical doublet, the two bypassed resonators are coupled inductively to each other. This is due to the narrow septum placed between the two fins to reduce the coupling between them; the approach allows us to place the two fins closer to one another thus saving space in comparison with the configuration without the narrow septum.

Frequency response of a typical E-plane waveguide doublet is demonstrated in Fig. 4.

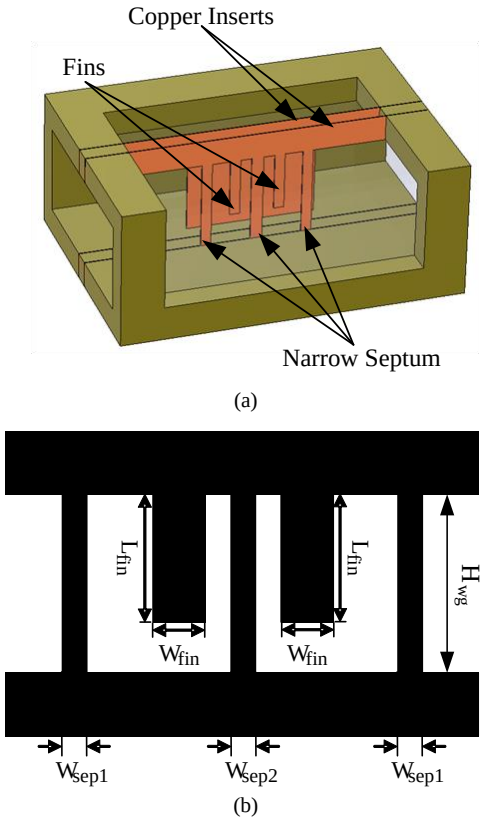


Fig. 3. Configuration of an E-plane doublet: (a) arrangement of the E-plane inserts within the waveguide housing; (b) configuration of the insert with the narrow septum.

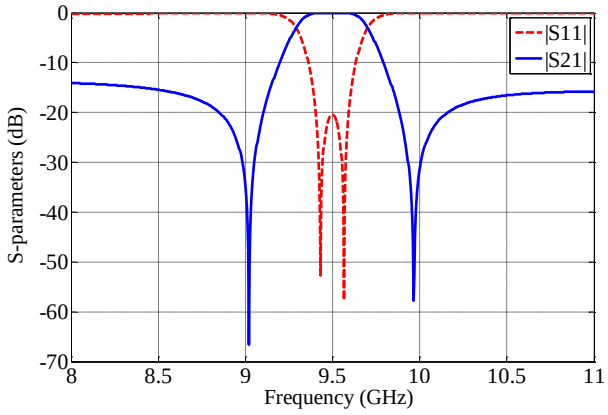


Fig. 4. Frequency response of the E-plane waveguide doublet.

## III. Extraction of Generalized Coupling Coefficients of the Filtering Blocks

In this section, we will address the problem of the generalized coupling coefficients (GCCs) extraction from the EM-simulated responses for symmetric singlet and doublet filtering blocks connected in series with extracted poles sections (EPS). For this purpose, we extract the GCCs of the individual blocks (singlets, doublets and EPS), separately.

### *A. GCC Extraction for Singlets*

Consider a symmetric singlet, illustrated by a coupling scheme in Fig. 5, which contains a resonator and two non-resonating nodes connected through admittance inverters. Taking advantage of the symmetry of the scheme, the circuit can be analysed by the even-odd mode technique. The short and open schematic circuits of the singlet, corresponding to the even and odd modes respectively, are shown in Fig. 6. Therefore, the input admittances for the both cases can be calculated as:

$$Y_{in,e} = -j\frac{1}{Q_e} \tag{1}$$

$$Y_{in,o} = -j\frac{1}{Q_o}\cdot\frac{\omega-\Omega_{Zo}}{\omega-\Omega_{Po}} \tag{2}$$

Here $\omega$ is a lowpass prototype frequency variable obtained from the real frequency $f$ by the standard bandpass to lowpass transformation, and the other entries are expressed through the circuit element values:

$$Q_e = \frac{B_N + J_N}{J_{in}^2} \tag{3}$$

$$Q_o = \frac{B_N - J_N}{J_{in}^2} \tag{4}$$

$$\Omega_{Po} = -B_1 + \frac{2\cdot J_{N1}^2}{B_N - J_N} \tag{5}$$

$$\Omega_{Zo} = -B_1 \tag{6}$$

It can be shown by expressing $S_{21}$ through the even-mode and odd-mode admittances that the doubly-loaded singlet has a finite transmission zero at $\Omega_{TZ}$:

$$\Omega_{TZ} = -B_1 - \frac{J_{N1}^2}{J_N} \tag{7}$$

Combining eq. (3)-(7), we obtain the ratios which completely determine the circuit of interest with respect to a scaling factor:

$$\frac{B_N}{J_{in}^2} = \frac{1}{2}\left(Q_e + Q_o\right) \tag{8}$$

$$\frac{J_N}{J_{in}^2} = \frac{1}{2}\left(Q_e - Q_o\right) \tag{9}$$

$$B_1 = -\Omega_{Zo} \tag{10}$$

$$\frac{J_{N1}^2}{B_N} = \left(\frac{2}{\Omega_{Po}-\Omega_{Zo}} + \frac{1}{\Omega_{Zo}-\Omega_{TZ}}\right)^{-1} \tag{11}$$

$$Q_{ext} = \frac{B_N}{J_{in}^2} = \frac{1}{2}\left(Q_e + Q_o\right) \tag{12}$$

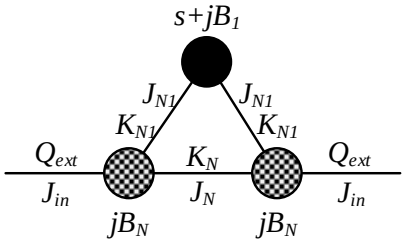


Fig. 5. Coupling scheme of a symmetric singlets. Solid nodes represent the resonators; patterned nodes are the non-resonating nodes; black lines represent admittance inverters (with values denoted as $J$). The corresponding GCC are denoted as $k$ and $Q_{ext}$.

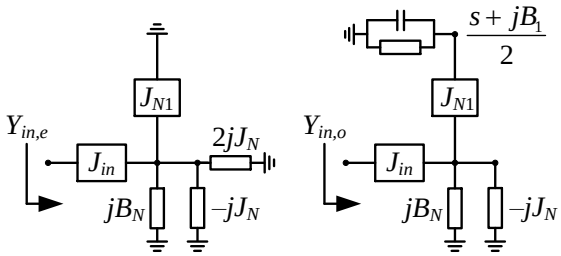


Fig. 6. Analysis of the symmetric singlet using the even-odd mode technique: short and open schematic circuits.

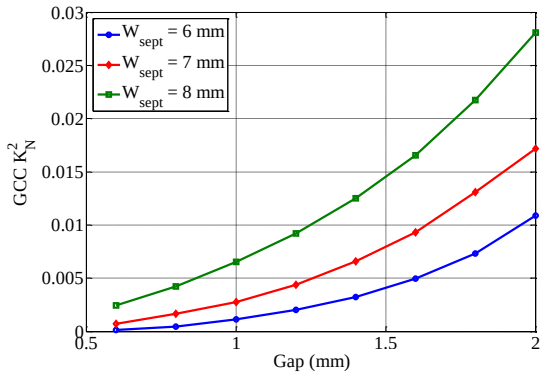


(a)

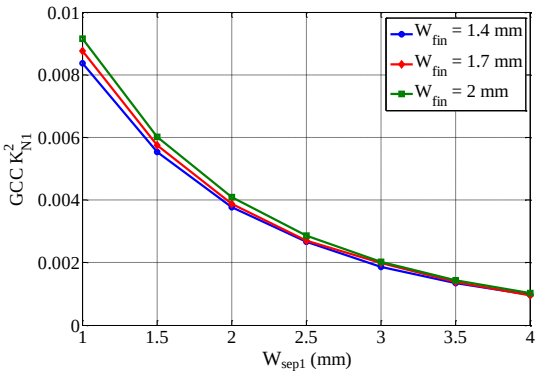


(b)

Fig. 7. Extracted generalized coupling coefficients of the E-plane waveguide singlet: (a) $K_N^2$; (b) $K_{N1}^2$.

The GCC $K_N$, $K_{N1}$ and $Q_{ext}$ are straightforwardly calculated from the above equations.

As an example, the extracted GCCs $K_N$ and $K_{N1}$ for a singlet designed at 9.2 GHz with 0.2 GHz bandwidth are presented in Fig. 7.

### *C. GCC Extraction for Symmetric Doublets*

Let us consider a symmetric doublet comprised of two resonating and two non-resonating nodes connected through admittance inverters, as illustrated by a coupling scheme presented in Fig. 8. The symmetric circuit is also analysed by the even-odd mode technique; the corresponding short and open circuits are shown in Fig. 9.

The even-mode input admittance $Y_{in,e}$ is expressed as follows:

$$Y_{in,e} = \frac{J_{in}^2}{j(B_N + J_N) + \dfrac{J_{N1}^2}{s + j(B_1 + J_1)}} \tag{13}$$

where $s = j\omega$.

The above admittance $Y_{in,e}$ is purely imaginary, it has a pole and a transmission zero denoted as $\Omega_{Pe}$ and $\Omega_{Ze}$ respectively:

$$Y_{in,e} = -j\frac{1}{Q_e}\cdot\frac{\omega - \Omega_{Ze}}{\omega - \Omega_{Pe}} \tag{14}$$

where

$$\Omega_{Pe} = -B_1 - J_1 + \frac{J_{N1}^2}{B_N + J_N} \tag{15}$$

$$\Omega_{Ze} = -B_1 - J_1 \tag{16}$$

$$Q_e = \frac{B_N + J_N}{J_{in}^2} \tag{17}$$

Once the pole and zero values are known, the external quality factor for the even-mode case $Q_e$ can be calculated at any frequency except of $\Omega_{Pe}$ and $\Omega_{Ze}$. For simplicity, we take $\omega = 0$ leading to:

$$Q_e = \frac{1}{\left|Y_{in,e}(\omega = 0)\right|}\cdot\frac{\Omega_{Ze}}{\Omega_{Pe}} \tag{18}$$

Similarly, the following set of equations can be obtained for the odd-mode input admittance:

$$Y_{in,o} = -j\frac{1}{Q_o}\cdot\frac{\omega - \Omega_{Zo}}{\omega - \Omega_{Po}} \tag{19}$$

$$\Omega_{Po} = -B_1 + J_1 + \frac{J_{N1}^2}{B_N - J_N} \tag{20}$$

$$\Omega_{Zo} = -B_1 + J_1 \tag{21}$$

$$Q_o = \frac{B_N - J_N}{J_{in}^2} \tag{22}$$

The odd-mode external Q-factor is extracted as:

$$Q_o = \frac{1}{\left|Y_{in,o}(\omega = 0)\right|}\cdot\frac{\Omega_{Zo}}{\Omega_{Po}} \tag{23}$$

The unknown ratios between the circuit model parameters, which completely characterize the schematic circuit model of the doublet structure, are obtained by combining the equations (15)-(17) and (20)-(22):

$$B_1 = -\frac{1}{2}\left(\Omega_{Zo} + \Omega_{Ze}\right) \tag{24}$$

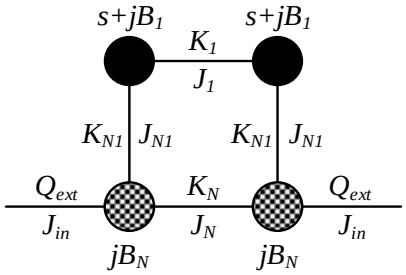


Fig. 8. Coupling scheme of a symmetric doublet.

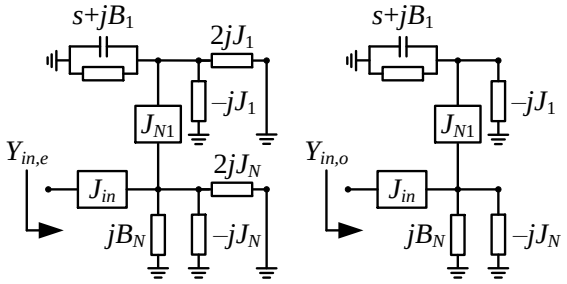


Fig. 9. Analysis of the symmetric doublet using the even-odd mode technique: short and open schematic circuits.

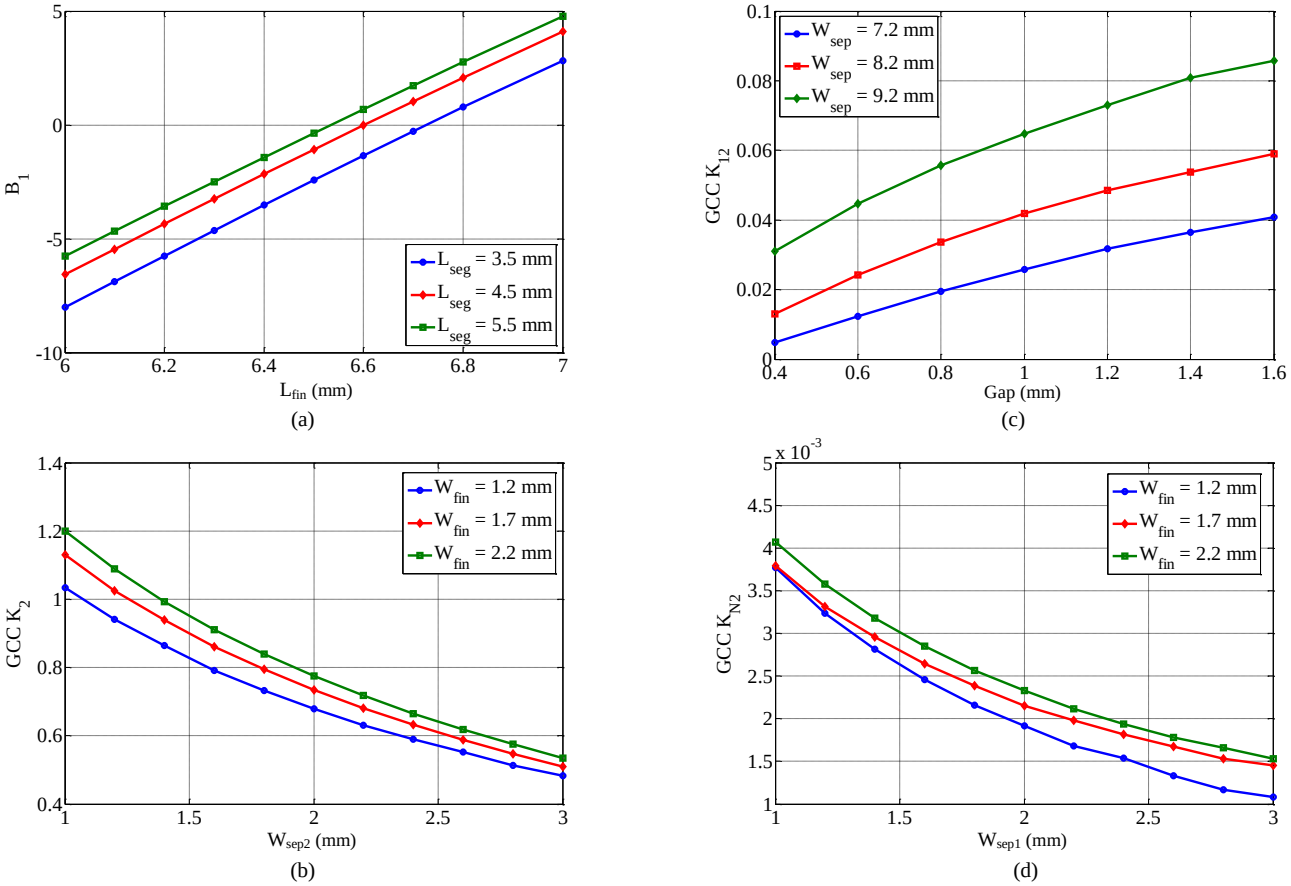


Fig. 10. Extracted generalized coupling coefficients of the E-plane waveguide doublet: (a) $B_1$ vs. $L_{fin}$; (b) $K_2$ vs. $W_{sep2}$; (c) $K_{12}$ vs. *Gap*; (d) $K_{N2}$ vs. $W_{sep1}$.

$$J_1 = \frac{1}{2}\left(\Omega_{Zo} - \Omega_{Ze}\right) \tag{25}$$

$$\frac{J_{N1}^2}{B_N} = 2\cdot\left(\frac{1}{\Omega_{Pe} - \Omega_{Ze}} + \frac{1}{\Omega_{Po} - \Omega_{Zo}}\right)^{-1} \tag{26}$$

$$\frac{J_{N1}^2}{J_N} = 2\cdot\left(\frac{1}{\Omega_{Pe} - \Omega_{Ze}} - \frac{1}{\Omega_{Po} - \Omega_{Zo}}\right)^{-1} \tag{27}$$

$$\frac{B_N}{J_{in}^2} = \frac{1}{2}\left(Q_e + Q_o\right) \tag{28}$$

$$\frac{J_N}{J_{in}^2} = \frac{1}{2}\left(Q_e - Q_o\right) \tag{29}$$

The GCCs $K_1 = J_1$, $K_N = J_N / B_N$, $K_{N1} = J_{N1}/\sqrt{B_N}$ are calculated from (24)-(29) by setting an arbitrary value of $J_{in}$, for example, unity. The plots in Fig. 10 has been obtained taking into consideration of the configuration of filter inserts shown in section II.*B*. The procedure for determination of the initial dimensions of the two inserts that form the doublet section is processed as follows. First the length of the metallic fin in varied while all other dimensions are kept constant until the required susceptance value $B_2$ is extracted. In order to extract the coupling coefficient $K_{N2}$, the width of septa ($W_{sep1}$) is adjusted while all other dimensions are kept constant. Coupling coefficient $K_2$ is extracted next by varying $W_{sep2}$. Following this the gap in the wide metallic fin in the second insert is adjusted until the required value for $K_{12}$ is extracted. It should be mentioned at this point that this method of obtaining physical dimensions does not provide the final solution. However, it endows the initial point at which further fine tuning, either manually or through an optimizer, will be required to achieve the final result. If an optimizer is to be

used, it provides the optimization process with certainty of finding acceptable results.

## IV. Proposed Filters

In order to illustrate the application of the proposed resonators for compact filters, three different filter structures are presented. The first example is a 3rd-order filter which consists of two EPS cascaded with a singlet, whereas the second example is a 4th-order filter consisting of two EPS cascaded with a doublet section. The third filter consists of three directly coupled resonators bypassed between source and load. The following subsections will detail the design of these filters.

### A. Filter I: Compact 3rd-order Filter

The design of the proposed third order filter includes a single E-plane EPS cascaded onto either side of a singlet. The E-plane EPS are created by modifying the existing conventional E-plane resonators via the inclusion of a single metallic fin, located between the two septa and grounded on one side through the top wall of the waveguide housing.

The schematic representation of an EPS contains a resonator connected through an inverter with a frequency invariant reactance (FIR) element, as shown in Fig. 11a. The shunt FIR element is referred to as a non-resonating node (NRN). In the examples to follow, the NRN is a node that resonates at frequencies much higher than the operating frequency of the filter. It is implemented physically in the following examples as a strongly detuned conventional E-plane resonator. A similar representation of an EPS is shown Fig. 11b, which is given as a coupling scheme composed of two nodes: resonating and non-resonating. The lines connecting nodes represent inverters. Detail analysis and design of filters based on cascaded E-plane EPS can be found in [10]. The arrangement of the two inserts to form the complete filter structure is shown in Fig. 12.

A single extracted pole section has the capability to produce a single pole ($\Omega_P$).and a transmission zero at ($\Omega_Z$), locations of which are described by equations (30) and (31).

$$\Omega_Z = -B_1, \tag{30}$$

$$\Omega_P = -B_1 + \frac{J_1^2}{B_N} \tag{31}$$

The set of equations above also shows that, in order to place the transmission zero below the passband the susceptance of the non-resonating node must be of positive sign. The coupling schematic of a third order filter with mixed topology is shown in Fig. 13.

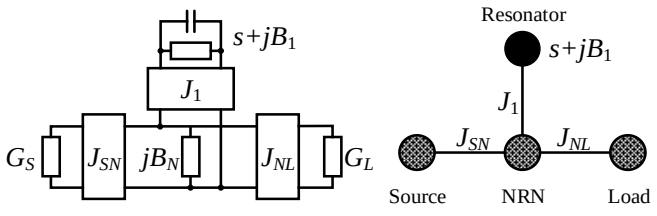


Fig. 11. E-plane extracted pole section: (a) schematic representation; (b) coupling scheme representation.

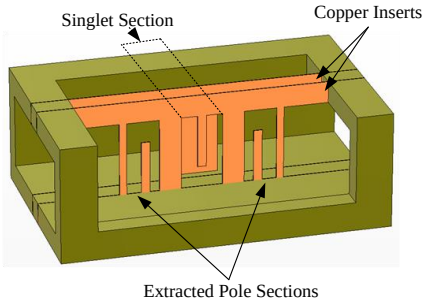


Fig. 12. Arrangement of E-plane inserts for the compact 3rd order cross coupled filter.

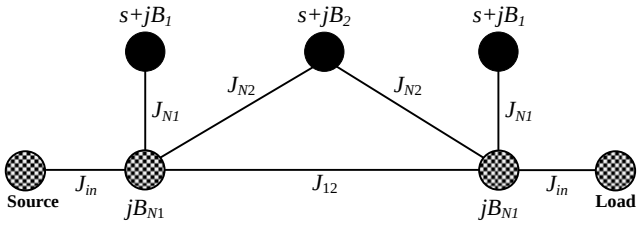


Fig. 13. Schematic representation of the compact 3rd order filter with mixed coupling topologies.

In order to demonstrate the performance of the proposed structure, the third order filter in Fig. 9 has been designed to satisfy the following specifications.

- Center frequency: 9.2 GHz;
- Ripple bandwidth: 0.2 GHz;
- Return loss: 20 dB;
- Transmission zeros (GHz):8.9, 9.9, 9.9.

First, the characteristic filter polynomials $E(s)$, $F(s)$ and $P(s)$ which correspond to the $S_{21}$ and $S_{11}$ rational functions have been derived using the recursive technique in [14]. Subsequently, the direct synthesis technique for inline filters with non-resonating nodes [15] has been applied in order to calculate the element values of the extracted pole sections.

$$S_{11} = \frac{F(s)}{E(s)_1}, \quad S_{21} = \frac{P(s)}{\varepsilon \,.\, E(s)}, \quad \varepsilon = 29.921 \tag{32}$$

$$P(s) = s^3 - j10.4545s^2 - 4.3956s \; - j139.095 \tag{33}$$

$$F(s) = s^3 + j0.0196s^2 + 0.7596s \; - j0.00954 \tag{34}$$

$$E(s) = s^3 + (2.2301 + j0.0160)s^2 + (3.3853 + j0.08231)s + (2.5830 - j0.12742) \tag{35}$$

At the end of the synthesis process, we are left with the following values for the elements in the coupling schematic as shown in Fig. 13: $J_{in} = 1$, $J_{12} = -0.3954$, $J_{N1} = 4.8983$, $J_{N2} = 0.885$, $B_{N1} = -4.5810$, $B_1 = -5.4020$, $B_2 = 0.50901$.

### B. Filter II: Compact 4th-order Filter

This subsection presents development of a 4th-order ultra-compact cross-coupled filter utilizing two extracted pole sections together with the proposed doublet in section II.*B*. The configuration of the filter inside waveguide housing is shown in Fig. 14. The lowpass prototype network that represents the proposed structure is given in Fig. 15.

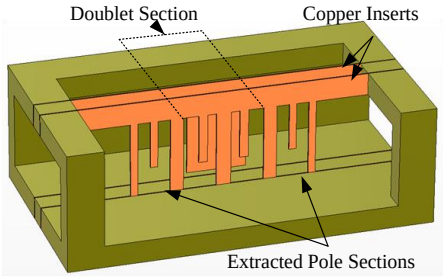


Fig. 14. Arrangement of E-plane inserts for the compact 4th-order cross-coupled filter.

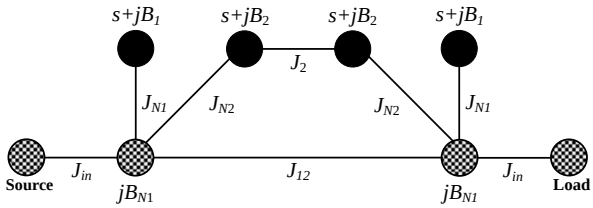


Fig. 15. Schematic representation of the 4th-order compact cross-coupled filter.

As an example to demonstrate the performance of the 4th-order cross-coupled filter, the structure in Fig. 14 was designed and simulated for the following specifications:

- Center frequency: 10 GHz;
- Ripple bandwidth: 0.25 GHz;
- Return loss: 20 dB;
- Transmission zeros (GHz): 9.5, 10.5, 10.5, 10.5.

The characteristic filter polynomials $E(s)$, $F(s)$ and $P(s)$ which corresponds to the $S_{21}$ and $S_{11}$ rational functions are given in equation (36)-(38).

$$P(s) = s^4 - j7.61s^3 + 2.35s^2 - j128.24s - 244.41 \quad (36)$$

$$F(s) = s^4 - j0.267s^3 + 0.981s^2 - j0.201s + 0.115 \quad (37)$$

$$E(s) = s^4 + (2.137 - j0.267)s^3 + (3.263 - j0.656)s^2 + (2.752 - j0.997)s + (1.115 - j0.731) \quad (38)$$

$$\varepsilon = 184.0341$$

The following values for the elements of the schematic in Fig. 15 were obtained at the end of the synthesis process: $J_{in} = 1$, $J_{N1} = 4.0301$, $J_{N2} = 0.8719$, $J_{12} = -0.0364$, $J_2 = 0.7179$, $B_{N1} = -3.8665$, $B_1 = -4.2848$, $B_2 = 0.0442$.

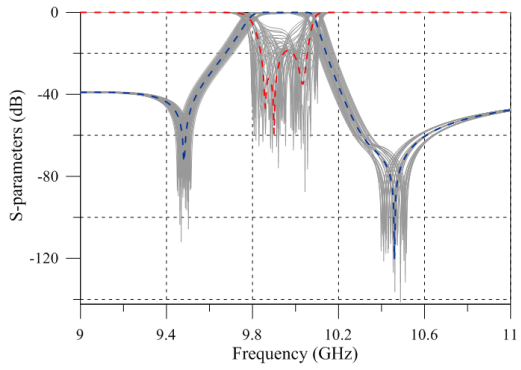


Fig. 16. Tolerance analysis (±50 µm) on insert dimensions (lengths and widths of metallic fins) of the proposed 4th-order cross-coupled filter.

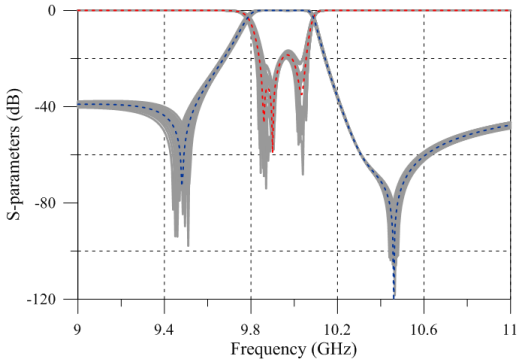


Fig. 17. Tolerance analysis (±100 µm) with respect to the alignment between the two inserts as well as the inserts and the housing of the proposed 4th-order cross-coupled filter.

A sensitivity analysis with a tolerance limit of ±50 µm with respect to the insert dimensions (lengths and widths of fins) and ±100 µm with respect to the alignment between the two inserts, as well as the inserts and the side walls, has been performed. The results obtained are provided in Fig. 16 and Fig. 17. It can be observed that the proposed structure is quite sensitive to variation in the insert dimension, especially the length of the metallic fins which forms the resonators.

### *C. Filter III: 3rd Order Filter Using Source-Load Coupling*

This subsection presents a third order filter with source-load coupling. The filter is formed by simply extending the singlet section described previously, where one of the inserts consists of a single wide septum, and the other consists of three parallel fins short-circuited on alternating sides, like in an interdigital array. Furthermore, narrow septa are placed coplanar between the fins, helping to reduce unwanted cross couplings between adjacent resonators. Consequently, the fins can be shifted much closer to each other and in return contributing towards reduction of the overall length of the structure.

In terms of equivalent circuit, as stated previously, the wide septum forms bifurcated waveguide section with couplings to the source and load being effectively inductive waveguide discontinuities in the form of H-plane steps [16]. Likewise, septa between resonators can be viewed as inductive discontinuities, forming inverters when absorbing additional

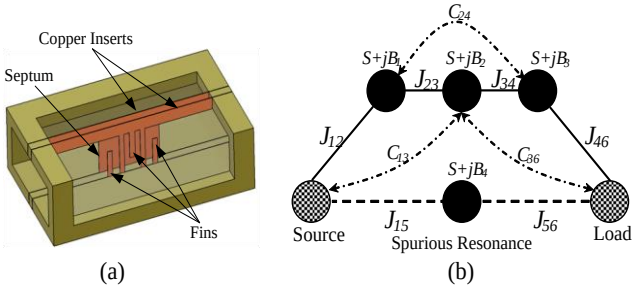


Fig. 18. A 3rd-order compact filter: (a) arrangement of E-plane inserts within a waveguide housing; (b) coupling schematic taking into account spurious resonance.

waveguide sections around them. Resonators themselves can be locally modelled as stripline quarter-wavelength resonators. Finally, the wide septum determines the bypass path to behave as inductive coupling.

The configuration and the coupling scheme of the proposed structure, taking into consideration the spurious resonance, is shown in Fig. 18a and Fig. 18b. However, this additional spurious resonant node could be ignored if only the response surrounding the pass band is of interest [17]. Symbols $C_{13}$, $C_{24}$, and $C_{36}$ represent additional parasitic couplings that may exist within the structure.

The coupling matrix for a third order filter that was designed at the centre frequency of 9.4 GHz with 0.5 GHz bandwidth and a transmission zero at 10.4 GHz has been obtained through an optimization routine and is given as:

$$M = \begin{bmatrix} 0 & 0.888 & 0.024 & 0 & 0.145 & 0 \\ 0.888 & 0 & 0.672 & 0.042 & 0 & 0 \\ 0.024 & 0.672 & 0 & 0.672 & 0 & 0.024 \\ 0 & 0.042 & 0.672 & 0 & 0 & 0.888 \\ 0.145 & 0 & 0 & 0 & -14.4 & 0.145 \\ 0 & 0 & 0.024 & 0.888 & 0.145 & 0 \end{bmatrix} \quad (39)$$

## V. RESULTS

Three ultra-compact waveguide filters (centre frequencies: 9.2 GHz, 10 GHz, and 9.4 GHz) with cross coupling have been designed in CST Microwave Studio™ and fabricated using the E-plane technology, which utilizes a pair of copper inserts within a standard WR-90 (22.86x10.16 mm$^2$) rectangular waveguide housing.

The inserts in Fig. 19-22, with the dimensions given in Tables I-III have been plotted on a copper foil with 0.1 mm thickness. S-parameters have been measured using the Agilent E8361A vector network analyzer. Comparison of the results obtained from schematic, simulation and measurements for the three structures are given in Fig. 23-25.

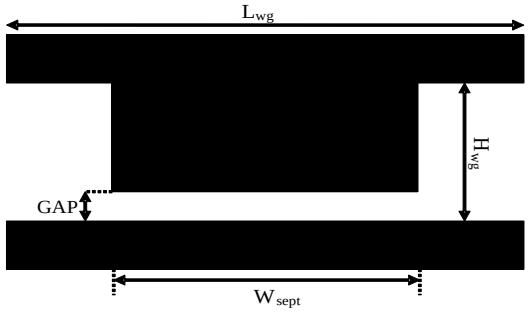


Fig. 19. Layout of the E-plane insert for cross-coupling in all three proposed filters.

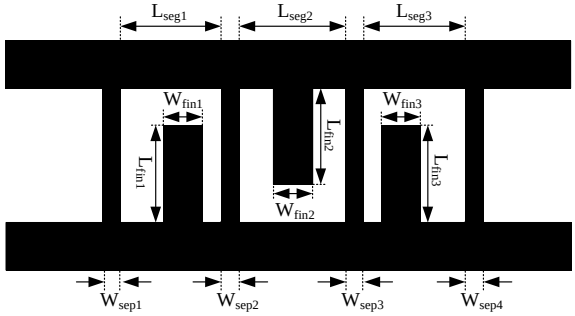


Fig. 20. Layout of the second E-plane insert for the proposed Filter I (section IV.*A*).

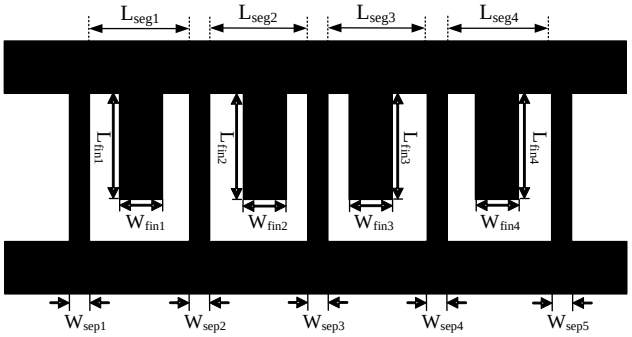


Fig. 21. Layout of the second E-plane insert for the proposed Filter II (section IV.*B*).

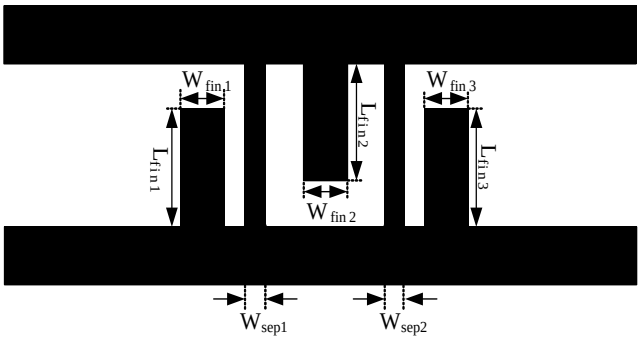


Fig. 22. Layout of the second E-plane insert for the proposed Filter III (section IV.*C*).

TABLE I
DIMENSIONS (IN MM) OF THE INSERTS (FIG. 19 AND FIG. 20) FOR FILTER I

| Parameters | Optimised values | Parameters | Optimised Values |
|---|---|---|---|
| $L_{fin1}$ | 6.99 | $W_{fin3}$ | 1.7 |
| $L_{fin2}$ | 6.97 | $W_{sept}$ | 6.0 |
| $L_{fin3}$ | 6.99 | $W_{sep1}$ | 1.0 |
| $L_{seg1} = L_{seg3}$ | 4.21 | $W_{sep2}$ | 2.3 |
| $L_{seg2}$ | 6.80 | $W_{sep3}$ | 2.3 |
| $W_{fin1}$ | 1.7 | $W_{sep4}$ | 1.0 |
| $W_{fin2}$ | 1.7 | *GAP* | 1.0 |

TABLE II
DIMENSIONS (IN MM) OF THE INSERTS (FIG. 19 AND FIG. 21) FOR FILTER II

| Parameters | Optimised values | Parameters | Optimised Values |
|---|---|---|---|
| $L_{fin1} = L_{fin4}$ | 6.41 | $W_{sept}$ | 8.2 |
| $L_{fin2} = L_{fin3}$ | 6.60 | $W_{sep1}$ | 1.0 |
| $L_{seg1} = L_{seg4}$ | 4.45 | $W_{sep2}$ | 1.8 |
| $L_{seg2} = L_{seg3}$ | 4.55 | $W_{sep3}$ | 2.0 |
| $W_{fin1}$ | 1.0 | $W_{sep4}$ | 1.8 |
| $W_{fin2}$ | 1.2 | $W_{sep5}$ | 1.0 |
| $W_{fin3}$ | 1.2 | *GAP* | 0.7 |
| $W_{fin4}$ | 1.0 | - | - |

TABLE III
DIMENSIONS (IN MM) OF THE INSERTS (FIG. 19 AND FIG. 22) FOR FILTER III

| Parameters | Optimised values | Parameters | Optimised Values |
|---|---|---|---|
| $L_{fin1}$ | 6.4 | $W_{fin3}$ | 1.6 |
| $L_{fin2}$ | 6.5 | $W_{sept}$ | 20.5 |
| $L_{fin3}$ | 6.4 | $W_{sep1}$ | 1.6 |
| $W_{fin1}$ | 1.6 | $W_{sep2}$ | 1.6 |
| $W_{fin2}$ | 1.6 | *GAP* | 0.0 |

Taking into consideration the inaccuracies of some of the dimensions during fabrication of the waveguide housing which was hand crafted, the measured results show good agreement with that of the simulated. The insertion losses for the three filters of around 1.5 dB for the fabricated filters described in section IV.*A*-*B* and 1.0 dB for the fabricated filter described in section IV.*C*, that can be observed in Fig. 21-23, are mainly due to signal leakage through the imperfect custom made waveguide housing. A slight shift in the transmission zeros can also be observed for the Filter III which is mainly due to inaccuracies of the inner channel dimensions. Further contributions to these are imperfections in alignment of the two inserts within the waveguide housing and tolerances encountered during fabrication process such as the limitation to accuracy which the plotter reaches. A sensitivity analysis with a tolerance limit of ±50μm with respect to the insert dimensions and ±100μm with respect to the alignment between the two inserts as well as the inserts and the side walls has been provided for the Filter II in order to demonstrate feasibility of these proposed filters. Measured results of the proposed filters can be further improved through meticulous use of the available tools and through an accurate construction of the waveguide housing using precision equipment.

Photographs of the three fabricated filter prototypes are shown in Figs. 26, 27 and 28 respectively.

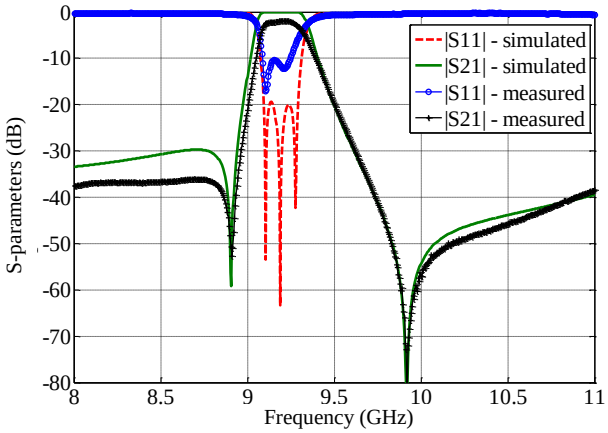


Fig. 23. Simulated and measured frequency responses of Filter I.

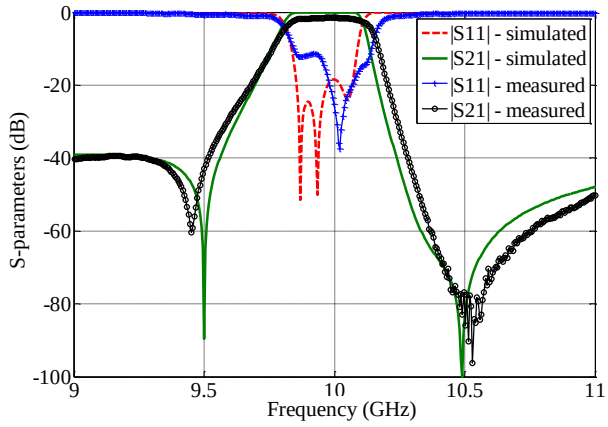


Fig. 24. Simulated and measured frequency responses of Filter II.

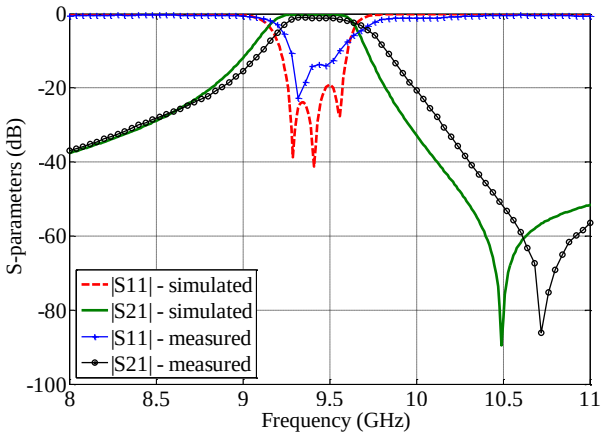


Fig. 25. Simulated and measured frequency responses of Filter III.

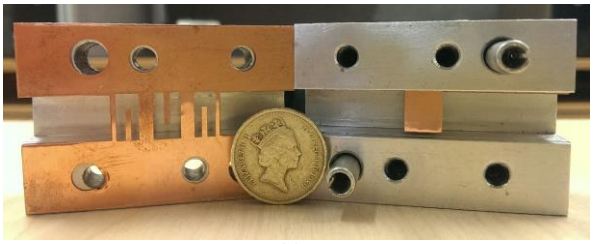

Fig. 26. View of fabricated Filter I.

Fig. 27. View of fabricated Filter II.

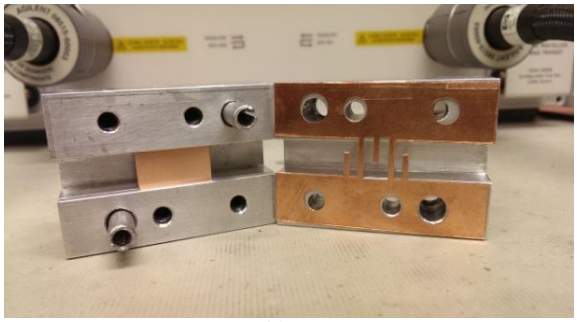

Fig. 28. View of fabricated Filter III.

TABLE IV
COMPARISON OF THE PROPOSED FILTERS
WITH CONVENTIONAL E-PLANE WAVEGUIDE FILTERS[1]

| Filter Description | $F_c$, GHz | *BW*, GHz | Total Insert Length, mm |
|---|---|---|---|
| Conventional 3rd-order filter | 9.2 | 0.2 | 71.7 |
| Proposed 3rd-order Filter I (see IV.*A*) | 9.2 | 0.2 | 21.8 |
| Conventional 4th-order filter | 10 | 0.25 | 98.6 |
| 4th-order EPS filter | 10 | 0.25 | 39.1 |
| Proposed 4th-order Filter II (see IV.*B*) | 10 | 0.25 | 25.6 |
| Conventional 3rd-order filter | 9.4 | 0.5 | 62.6 |
| Proposed 3rd-order Filter III (see IV.*C*) | 9.4 | 0.5 | 20.5 |

[1] $F_c$ – center frequency, *BW* – bandwidth

TABLE V
Q-FACTORS COMPARISON
BETWEEN PROPOSED AND CONVENTIONAL RESONATORS

| Resonator type | Unloaded Q-factor ($Q_U$) |
|---|---|
| Conventional E-plane resonator | 5991 |
| E-plane EPS | 4449 |
| Proposed E-plane singlet | 3962 |
| Proposed E-plane doublet | 3130 and 2898 |

## VI. DISCUSSION

### A. Size and Losses

In order to demonstrate size reduction achieved by the proposed filters, we designed four E-plane filters with identical specifications using traditional approaches, such as [7] and [10]. Comparison between the sizes of conventional, E-plane EPS and proposed filters is provided in Table IV. It is evident that the proposed structures are approximately 70-74% more compact comparing to a conventional E-plane filter with similar response and 35% smaller than standard E-plane extracted pole filters of the same order. Additionally, the filters have improved upper and lower stop band selectivity due to a transmission zero generated through source-load, or inter resonator cross coupling.

For each one of these sections, we used the Eigen-mode solver in CST Microwave Studio™ to compute their resonant frequencies and the corresponding electromagnetic field patterns with no excitation applied. Subsequently, we estimated unloaded quality factors ($Q_U$) through the inbuilt tool for loss and Q calculation using the obtained field solutions. Table V summarises the *Q*-factors of a conventional E-plane resonator, E-plane EPS, proposed singlets and doublets. One can see that the $Q_U$ of the proposed structures dropped by 34% for the singlet and almost by 50% for the doublet comparing to the conventional E-plane resonator. In other words, the size reduction has been achieved at the cost of increased losses. However, it should be remarked that the estimated *Q*-factors of the presented structures are still high.

### B. Limitations

It is possible to design filters with wider bandwidths using the proposed approach. However, this results in narrowing of the septa as well as the fins in order to obtain the required couplings. For a filter designed for a centre frequency of 9.7 GHz with 12% fractional bandwidth, the widths of the metallic fins and the septa are 0.5 mm and 0.7 mm respectively. Any further increase in fractional bandwidth would lead to further narrowing of these dimensions. Therefore the bandwidth limitation is due to physical realisation of the filter dimensions.

## VII. CONCLUSION

In this paper, we have proposed novel ultra-compact E-plane waveguide filters that exhibit pseudo-elliptic frequency responses with ability to place transmission zeros in both the upper and lower stopbands. Three examples of such filters were given, two of which use extracted pole sections cascaded with proposed cross-coupled modules, whereas the third consists of three resonators bypassed between source and load. A GCC extraction procedure has been provided which can facilitate the development of these filters. A tolerance analysis conducted showed that the filters are sensitive to variation in the dimensions of fins which represent quarter-wave resonators. Inherently, proposed structures are more sensitive to fabrication tolerances in comparison to conventional E-plane filters. However, only the copper insert (which is cheap to fabricate) is needed to be changed in order to realise different filter characteristics. In order to validate the performance of these filters, they have been fabricated and tested. S-parameter responses of the fabricated prototypes show reasonably good agreement with that of the simulated, even considering low accuracies of the fabrication device used, especially when fabricating the custom aluminium split block waveguide housing.

## REFERENCES


[1] A.E. Atia, A.E. Williams, "Narrow-Bandpass Waveguide Filters," *IEEE Trans. Microw. Theory Techn.*, vol.20, no.4, pp.258-265, Apr 1972.

[2] S. Bastioli, C. Tomassoni, R. Sorrentino, "A New Class of Waveguide Dual-Mode Filters Using TM and Nonresonating Modes," *IEEE Trans. Microw. Theory Techn.*, vol.58, no.12, pp.3909-3917, Dec. 2010.

[3] C. Tomassoni, S. Bastioli, R. Sorrentino, "Generalized TM Dual-Mode Cavity Filters," *IEEE Trans. Microw. Theory Techn.*, vol.59, no.12, pp.3338-3346, Dec. 2011.

[4] Hai Hu; Ke-Li Wu; Richard J. Cameron, "A design technique for stepped circular waveguide dual-mode filters for broadband contiguous multiplexers," *Microwave Symposium Digest (MTT), 2011 IEEE MTT-S International* , vol., no., pp.1-4, 5-10 June 2011.

[5] L. Pelliccia, F. Cacciamani, C. Tomassoni, R. Sorrentino, "Ultra-compact filters using TM dual-mode dielectric-loaded cavities with asymmetric transmission zeros," *Microwave Symposium Digest (MTT), 2012 IEEE MTT-S International* , vol., no., pp.1-3, 17-22 June 2012.

[6] Hai Hu, Ke-Li Wu, "A $TM_{11}$ Dual-Mode Dielectric Resonator Filter With Planar Coupling Configuration," *IEEE Trans. Microw. Theory Techn.*, vol.61, no.1, pp.131-138, Jan. 2013.

[7] Y. Konishi, and K. Uenakada, "The Design of a Bandpass Filter With Inductive Strip Planar Circuit Mounted in Waveguide," *IEEE Trans. Microw. Theory Techn.*, vol. MTT-22, pp. 869-873, Oct.1974.

[8] E. Ofli, R. Vahldieck, S. Amari, "Novel E-plane filters and diplexers with elliptic response for millimeter-wave applications," *IEEE Trans. Microw. Theory Techn.*, vol.53, no.3, pp. 843-851, March 2005.

[9] N. Suntheralingham and D. Budimir, "Enhanced Waveguide Bandpass Filters Using S-shaped Resonators," *Int. J. RF and Microwave CAE*, vol. 19, no. 6, pp. 627-633, 2009.

[10] O. Glubokov, D. Budimir, "Extraction of Generalized Coupling Coefficients for Inline Extracted Pole Filters With Nonresonating Nodes," *IEEE Trans. Microw. Theory Techn.*, vol.59, no.12, pp.3023-3029, Dec. 2011.

[11] N. Mohottige, U. Jankovic, D. Budimir, "Ultra compact pseudo-elliptic inline waveguide bandpass filters using bypass coupling," *Microwave Symposium (IMS), 2014 IEEE MTT-S International* , vol., no., pp.1-4, 1-6 June 2014.

[12] S. Amari, U. Rosenberg, J. Bornemann, "Singlets, cascaded singlets, and the nonresonating node model for advanced modular design of elliptic filters," *Microwave and Wireless Components Letters, IEEE* , vol.14, no.5, pp.237-239, May 2004.

[13] S. Amari, U. Rosenberg, "A universal building block for advanced modular design of microwave filters," *Microwave and Wireless Components Letters, IEEE* , vol.13, no.12, pp. 541-543, Dec. 2003.

[14] R. J. Cameron, C. M. Kudsia, R. R. Mansour, *Microwave Filters for Communication Systems, Fundamentals, Design and Applications*, Hoboken, New Jersey, John Wiley & Sons, 2007.

[15] S. Amari, G. Macchiarella, "Synthesis of inline filters with arbitrarily placed attenuation poles by using nonresonating nodes," *IEEE Trans. Microw. Theory Techn.*, vol.53, no.10, pp.3075-3081, Oct. 2005.

[16] T. Itoh, Ed., *Numerical Techniques for Microwave and Millimeter-Wave Passive Structures*, Hoboken, New Jersey, Wiley-Blackwell, 1989.

[17] S. Amari, U. Rosenberg, "Characteristics of cross (bypass) coupling through higher/lower order modes and their applications in elliptic filter design," *IEEE Trans. Microw. Theory Techn.*, vol.53, no.10, pp.3135-3141, Oct. 2005.

**Nandun Mohottige** (S'11-M'16) received the B.Eng. degree in electronic engineering as well as the Ph.D. degree in electronic and computer science in from the University of Westminster, London, U.K., in 2010 and 2015 respectively.

Since 2011 he has been with the Wireless communications Research Group, Faculty of Science and Technology, University of Westminster. His main research interests include design and analysis of miniaturised waveguide filters.

**Oleksandr Glubokov** (S'10-M'11) received the B.Eng. and M.Sc. degrees in telecommunications from the National technical University of Ukraine, Kiev, Ukraine, in 2005 and 2007respectively. He received his PhD degree in electronic and electrical engineering at the University of Westminster, London, United Kingdom in 2011. In 2012-2014 he worked as a Postdoctoral Research Fellow at the Reykjavik University, Iceland. Oleksandr is currently working as a Post-doc on MEMS THz systems project with Micro- and Nanosystems at KTH. His research focus is sub- THz filter design and numerical Optimization of sub- THz circuits.

**Uros Jankovic** received the Dipl.-Ing. and M.Sc. degrees in electrical engineering and computer science from the University of Belgrade in 2011 and 2013, respectively. In November 2012, he joined the University of Westminster for doing his MRes dissertation. He is currently working towards the Ph.D. degree. His main area of research is waveguide filters.

**Djuradj Budimir** (M'93–SM'02) received the Dipl. Ing. and M. Sc. degrees in electronic engineering from the University of Belgrade, Belgrade, Serbia, and the Ph.D. degree in electronic and electrical engineering from the University of Leeds, Leeds, U.K. In March 1994, he joined the Department of Electronic and Electrical Engineering at Kings College London, University of London. Since January 1997, he has been with the Faculty of Science and Technology, University of Westminster, London, UK, where he is now a Reader of wireless communications and leads the Wireless Communications Research Group. His expertise includes design of circuits from RF through microwave to millimetre-wave frequencies for 4G, and 5G wireless communications, WLAN, WPAN, UWB, wireless sensors, Internet of Things (IoT) and biomedical applications. Dr Budimir has authored or coauthored over 300 papers in the most reputable journals such as *IEEE Transactions on Microwave Theory and Techniques*, and other prestigious journals and conferences. He is the author of the book Generalized Filter Design by Computer Optimization (Artech House, 1998) and Software and Users Manual EPFIL-Waveguide E-plane Filter Design (Artech House, 2000) and a chapter in the book Encyclopedia of RF and Microwave Engineering (Wiley, 2005). He serves as an Associate Editor for Electronic Letters and a senior member of IEEE. He is a local co-chair of European Microwave Conference (EuMW2016) and member of the technical program committee of several conferences. He has won awards for his journal papers. Dr. Budimir is a Member of the EPSRC Peer Review College and a Charter Engineer.